Ligand Electronic Effects on Late Transition Metal Polymerization Catalysts

Christopher Popeney and Zhibin Guan*

Department of Chemistry, University of California, 516 Rowland Hall, Irvine, California 92697-2025

Received December 21, 2004

A series of bis-(aryl)-α-diimine ligands were synthesized bearing a range of electron-donating and -withdrawing substituents to systematically investigate the ligand electronic effects on late transition metal olefin polymerization catalysts. Their palladium(II) complexes were prepared and characterized. Electronic perturbations were verified by analysis of the ^{1}H and ^{13}C NMR chemical shifts of the corresponding methyl chloride complexes and the CO stretching frequencies of the corresponding cationic carbonyl complexes, which were found to correlate strongly with the Hammet substituent constant (σ_p) of the substituent on the ligand. The palladium(II) complexes of the functionalized α-diimine ligands were employed in the polymerization of ethylene and the copolymerization of ethylene with methyl acrylate. For ethylene homopolymerization, higher molecular weight was obtained with catalysts bearing more strongly electron-donating ligands. It was observed for the first time that the ligand electronic structure of the catalysts had a significant effect on topology of the polyethylene formed. More dendritic polyethylene was obtained with catalysts bearing more strongly electron-withdrawing ligands. This provides a fundamentally different approach (catalyst approach) to control polyolefin branching topology, which complements our previous strategy of controlling polymer topology by polymerization conditions. For the copolymerization of ethylene with methyl acrylate, strong correlations were observed in the incorporation ratio of methyl acrylate; catalysts bearing strongly electron-donating ligands afforded copolymers with higher incorporation of the polar comonomer. These catalysts also exhibited far greater activity in the presence of polar monomers than catalysts bearing more weakly donating ligands possessing withdrawing substituents, which were deactivated completely when methyl acrylate concentrations were sufficiently high.

Introduction

Recent interest in the development of late transition metal catalysts for the polymerization of olefins has been spurred by their high functional group tolerance and their ability to control polymer topology.[1−9] The Pd-(II) aryl-substituted α-diimine systems have received much attention because they allow precise control of polymer topology through simple variation of olefin feed concentration.[6−9] Branched polymer structures obtained by these catalysts are attributed to an isomerization mechanism, or "chain walking" of the catalyst along the polymer chain, operating in addition to the migratory insertion polymerization mechanism. One attractive feature of this system is its ability to prepare hyperbranched to dendritic polyethylene under conditions of low ethylene pressure.[6] The reduced oxophillicity of palladium endows the catalysts with the ability to produce copolymers with a variety of polar-functionalized olefins, allowing the preparation of complex functional polymer architectures in simple, one-pot syntheses.[10]

Since Brookhart's seminal discovery,[3,4] tremendous efforts have been spent in both industrial and academic laboratories on improving late transition metal catalyst systems. Many structural modifications, including steric tuning, changing the ligand backbone structure, and changing the chelating heteroatoms, have been pursued on the archetype α-diimine ligands.[1,2] However, an important parameter in catalyst design, the ligand electronic structure, has not been systematically investigated. Ligand electronic effects have been observed in many catalytic systems. For example, in hydrocarbon oxidation using iron porphyrin catalysts, a good Hammett correlation was observed for the oxidation product yields and the Hammett constants for the substituents on the porphyrin ligands.[11] In asymmetric catalysis,

* To whom correspondence should be addressed. E-mail: zguan@uci.edu.

(1) Ittel, S. D.; Johnson, L. K.; Brookhart, M. *Chem. Rev.* **2000**, *100*, 1169−1203, and references therein.
(2) Gibson, V. C.; Spitzmesser, S. K. *Chem. Rev.* **2003**, *103*, 283−315, and references therein.
(3) Johnson, L. K.; Killian, C. M.; Brookhart, M. *J. Am. Chem. Soc.* **1995**, *117*, 6414−6415.
(4) Johnson, L. K.; Mecking, S.; Brookhart, M. *J. Am. Chem. Soc.* **1996**, *118*, 267−268.
(5) Mecking, S.; Johnson, L. K.; Wang, L.; Brookhart, M. *J. Am. Chem. Soc.* **1998**, *120*, 888−899.
(6) Guan, Z.; Cotts, P. M.; McCord, E. F.; McLain, S. J. *Science* **1999**, *283*, 2059−2062.
(7) Cotts, P. M.; Guan, Z.; McCord, E.; McLain, S. *Macromolecules* **2000**, *33*, 6945−6952.
(8) Guan, Z. *Chem. Eur. J.* **2002**, *8*, 3086−3092.
(9) Guan, Z. *J. Polym. Sci. A: Polym. Chem.* **2003**, *41*, 3680−3692.
(10) Chen, G.; Ma, X. S.; Guan, Z. *J. Am. Chem. Soc.* **2003**, *125*, 6697−6704.

10.1021/om048988j CCC: $30.25
Publication on Web 02/12/2005

Chart 1

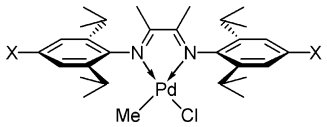

1: X = NO_2 **5**: X = Me
2: X = CF_3 **6**: X = OMe
3: X = Cl **7**: X = NMe_2
4: X = H

enantioselectivity was influenced by the ligand electronic structure of the catalysts.[12,13] A remarkable demonstration of ligand electronic tuning for improving catalytic activity is the development of the Grubbs ruthenium carbene metathesis catalysts.[14,15] For polymerization catalysis, significant ligand electronic effects were observed in a number of systems.[16−21] For example, Waymouth and co-workers discovered a profound ligand electronic effect on stereoselectivity in propylene polymerization using their "oscillating" zirconocene catalysts.[18] Coates and co-workers reported an order of magnitude increase of polymerization rate by placing a cyano group on the β-diiminate ligand for CO_2/epoxide copolymerization using β-diiminate zinc alkoxide catalysts.[21]

For α-diimine-based late transition metal complexes, ligand electronic effects manifested in a few reactions. For example, in C−H activation chemistry on arenes using α-bis(aryl)diimine complexes of platinum, electron-donating substituents on the ligand were found to increase the rate of activation.[22] Others have shown that incorporation of electron-donating or -withdrawing substituents onto α-diimine ligands affects their σ-donating ability to Pd(II) as well as the Lewis acidity of the metal.[23,24] For olefin polymerizations, Brookhart and co-workers observed an increase in polar olefin incorporation for increasingly electron-donating ligands.[5] Despite these studies, a thorough and systematic account of electronic effects on late transition metal α-diimine olefin polymerization catalyst systems has yet to be reported.

In this study, the preparation and polymerization properties of six new substituted Pd(II)-α-diimine complexes, **1**−**3** and **5**−**7** (Chart 1), are reported. In particular, the resulting effects upon polymer molecular weight, polymer branching topology, tolerance to polar monomers, and polar monomer incorporation are described. A specific interest we have in mind is to investigate the ligand electronic effects on the topology for polymers formed with the catalysts. Polymer branching topology is an important molecular parameter for controlling polymer physical properties. Our group has been developing efficient strategies for controlling polymer topology by using transition metal catalyzed polymerization.[8,9] Our previous strategy for controlling the topology of ethylene homopolymers and copolymers using the Brookhart Pd(II) catalyst system is based on the monomer concentration effect on polymerization kinetics.[6,10] In this study, we would like to examine the ligand electronic effects on polymerization kinetics and the resulting polymer topology. Our hypothesis is that the perturbation of electronic structure of the catalyst system should change the relative rate constants for insertion and chain walking ($k_{ins}/k_{walking}$), which will manifest in the resulting polymer topology.

Chart 2

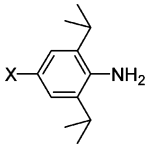

8: X = NO_2
9: X = NMe_2

Scheme 1

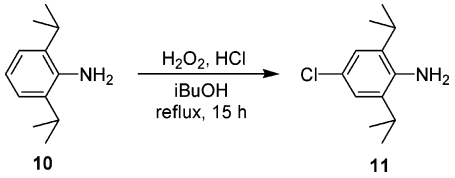

10 **11**

Scheme 2

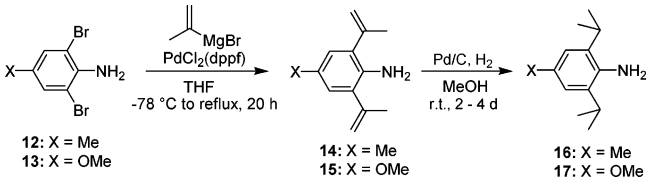

12: X = Me
13: X = OMe
14: X = Me
15: X = OMe
16: X = Me
17: X = OMe

Results and Discussion

A. Synthesis and Spectroscopic Studies of Substituted Pd(II) Complexes. Synthesis of Substituted α-Diimine Ligands. Substituents were placed in the *para*-aryl position on the α-diimine ligands, where the substituent could influence the donating ability of the ligand while not changing sterics at the metal center. The presence of *ortho*-isopropyl groups on the aryl rings of the ligands was necessary to block associative chain transfer during polymerization in order to produce high molecular weight polymer.[3] In the first step, corresponding substituted anilines possessing *ortho*-isopropyl groups were prepared for the α-diimine ligand synthesis.

Nitro- and dimethylamino-substituted anilines, **8** and **9** (Chart 2), were prepared using literature methods.[25] The *p*-chloride **11** was prepared from **10** by an oxidative chlorination route (Scheme 1).[26]

The remaining anilines were synthesized by Pd-catalyzed isopropylation of the 2,6-dibrominated *para*-substituted anilines. Palladium-catalyzed Kumada cou-

(11) Nappa, M. J.; Tolman, C. A. *Inorg. Chem.* **1985**, *24*, 4711−4719.
(12) RajanBabu, T. V.; Casalnuovo, A. L. *Pure Appl. Chem.* **1994**, *66*, 1535−1542.
(13) RajanBabu, T. V.; Casalnuovo, A. L.; Ayers, T. A.; Nomura, N.; Jin, J.; Park, H.; Nandi, M. *Curr. Org. Chem.* **2003**, *7*, 301−316.
(14) Trnka, T. M.; Grubbs, R. H. *Acc. Chem. Res.* **2001**, *34*, 18−29.
(15) Love, J. A.; Sanford, M. S.; Day, M. W.; Grubbs, R. H. *J. Am. Chem. Soc.* **2003**, *125*, 10103−10109.
(16) Lanza, G.; Fragala, I. L.; Marks, T. J. *J. Am. Chem. Soc.* **2000**, *122*, 12764−12777.
(17) Deming, T. J. *J. Am. Chem. Soc.* **1997**, *119*, 2759−2760.
(18) Lin, S.; Hauptman, E.; Lal, T. K.; Waymouth, R. M.; Quan, R. W.; Ernst, A. B. *J. Mol. Catal. A: Chem.* **1998**, *136*, 23−33.
(19) Kamigaito, M.; Lal, T. K.; Waymouth, R. M. *J. Polym. Sci. A: Polym. Chem.* **2000**, *38*, 4649−4660.
(20) Alcazar-Roman, L. M.; O'Keefe, B. J.; Hillmyer, M. A.; Tolman, W. B. *Dalton Trans.* **2003**, 3082−3087.
(21) Moore, D. R.; Cheng, M.; Lobkovsky, E. B.; Coates, G. W. *Angew. Chem., Int. Ed.* **2002**, *41*, 2599−2602.
(22) Zhong, H. A.; Labinger, J. A.; Bercaw, J. E. *J. Am. Chem. Soc.* **2002**, *124*, 1378−1399.
(23) Gasperini, M.; Ragaini, F.; Cenini, S. *Organometallics* **2002**, *21*, 2950−2957.
(24) Gasperini, M.; Ragaini, F. *Organometallics* **2004**, *23*, 995−1001.
(25) Carver, F. J.; Hunter, C. A.; Livingstone, D. J.; McCabe, J. F.; Seward, E. M. *Chem. Eur. J.* **2002**, *8*, 2848−2859.
(26) Vyas, P. V.; Bhatt, A. K.; Ramachandraiah, G.; Bedekar, A. V. *Tetrahedron Lett.* **2003**, *44*, 4085−4088.

Scheme 3

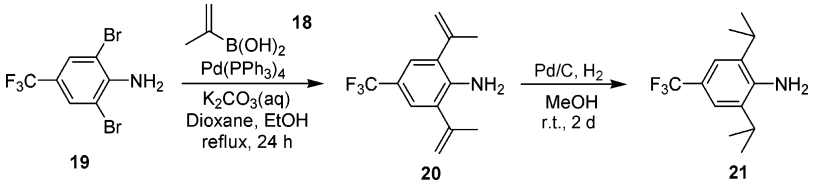

Scheme 4

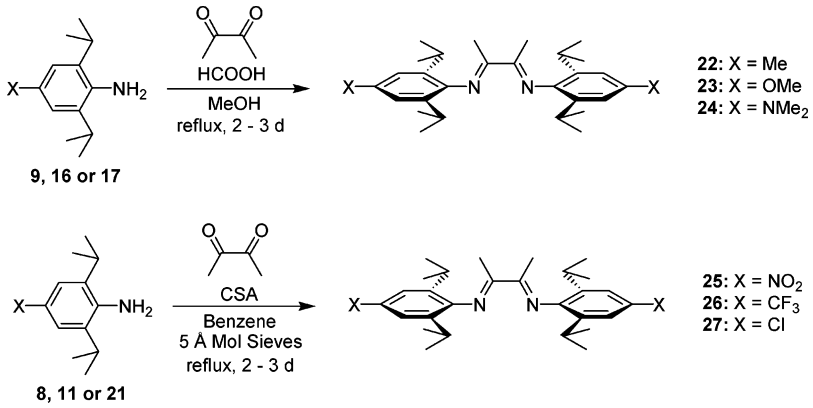

pling of Me- and OMe-substituted dibromoanilines **12** and **13** with isopropenylmagnesium bromide (Scheme 2) was effective in constructing the diisopropenyl adducts **14** and **15**.[27] Synthesis of **13** was achieved by the reaction of *para*-anisidine with an ammonium tribromide salt.[28]

Because the CF_3 group is sensitive to the Grignard reagent used in Kumada coupling, Suzuki coupling with isopropenylboronic acid **18** (Scheme 3) was utilized to give the CF_3-substituted diisopropenyl adduct **20**.[29] Hydrogenation of the crude diisopropenylated anilines **14**, **15**, and **20** was sluggish, presumably due to the poisoning of the Pd/C catalyst by the formed anilines, but the reaction was driven by periodically replenishing the catalyst. Hydrogenated anilines **16**, **17**, and **21** were used directly for the preparation of the corresponding α-diimines.

Electron rich α-diimine ligands **22**−**24** were prepared using mild condensation conditions: methanol at reflux with catalytic formic acid (Scheme 4).[30] Preparation of α-diimines **25**−**27** from electron-deficient anilines required azeotropic water removal from benzene using 5 Å molecular sieves for dehydration and 10-camphorsulfonic acid (CSA) as catalyst. Recrystallization of the ligands in methanol or ethanol afforded high-purity ligand in all cases except for diimine **23**.

Synthesis and Spectroscopic Studies of Pd(II)(α-diimine)MeCl Complexes 1−7 and [Pd(II)(α-diimine)Me(CO)]$^+$ Salts. Complexation of electron-rich and neutral α-diimines to Pd(II) proceeded by the displacement of 1,5-cyclooctadiene (COD) from Pd(COD)MeCl to afford complexes **3** and **5**−**7**.[31] The electron-poor ligands **25** and **26** displaced COD sluggishly so the corresponding Pd(II) complexes **1** and **2** were prepared by an in situ transmetalation−complexation protocol from the more reactive precursor $Pd(PhCN)_2Cl_2$.[32] The two methods are illustrated in Scheme 5.

Scheme 5

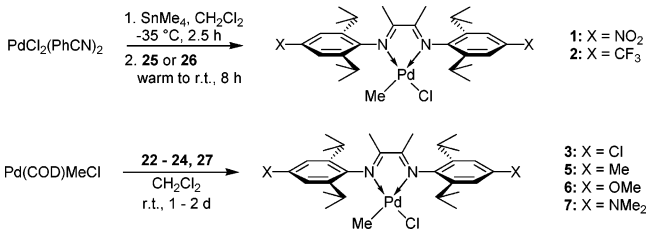

^{1}H and ^{13}C NMR analysis of the Pd-bound methyl groups (Pd-*Me*) in **1**−**7** indicated clear electronic effects. Figure 1 illustrates chemical shift trends versus the Hammett substituent constants (σ_p) of the ligand substituents.[33] Resonances were overall shifted downfield for complexes bearing withdrawing ligands and upfield for donating ligands. It is interesting to note an inversion point in the dependence of ^{1}H chemical shift upon the Hammet constant of the substituents. The most electron-rich complexes **6** and **7** exhibited resonances in ^{1}H NMR spectra that appeared more downfield than expected. We propose this results from two competing effects on the proton chemical shift: one is electronegativity effect and the second is magnetic anisotropy effect. As shown in X-ray crystal structures by Brookhart for a complex similar to **4**,[34] the methyl group is in the magnetic deshielding region of the two phenyl rings that are roughly perpendicular to the coordination plane. For the complexes containing strong electron-donating groups

(27) Bumagin, N. A.; Luzikova, E. V. *J. Organomet. Chem.* **1997**, *532*, 271−273.
(28) Kajigaeshi, S.; Kakinami, T.; Inoue, K.; Kondo, M.; Nakamura, H.; Fujikawa, M.; Okamoto, T. *Bull. Chem. Soc. Jpn.* **1988**, *61*, 597−599.
(29) Miyaura, N.; Yanagi, T.; Suzuki, A. *Synth. Commun.* **1981**, *11*, 513−519.
(30) Tom Dieck, H.; Svoboda, M.; Greiser, T. *Naturforschung* **1981**, *36B*, 823−832.
(31) Salo, E. V.; Guan, Z. *Organometallics* **2003**, *22*, 5033−5046.
(32) Vanasselt, R.; Gielens, E. E. C. G.; Rulke, R. E.; Vrieze, K.; Elsevier: C. J. *J. Am. Chem. Soc.* **1994**, *116*, 977−985.
(33) Hansch, C.; Leo, A.; Taft, R. W. *Chem. Rev.* **1991**, *91*, 165−195.
(34) Tempel, D. J.; Johnson, L. K.; Huff, R. L.; White, P. S.; Brookhart, M. *J. Am. Chem. Soc.* **2000**, *122*, 6686−6700.

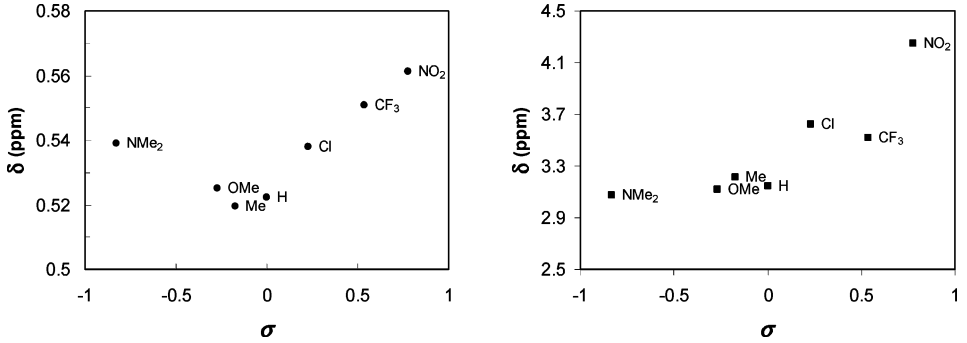

Figure 1. Chemical shifts for Pd-*Me* resonances of complexes **1**−**7** in ^{1}H NMR (left) and ^{13}C NMR (right).

Scheme 6

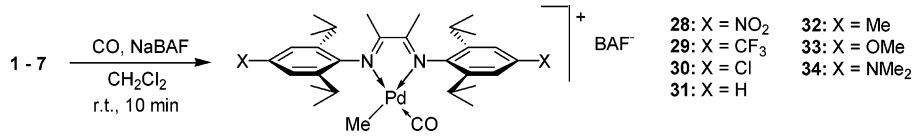

(**6** and **7**), the electron-rich aromatic rings lead to larger deshielding magnetic anisotropy effects from their ring current, which counterbalances the electronegativity effect and makes the ^{1}H chemical shift more downfield than expected. In support of this proposal, resonances of the methine protons (C*H*Me$_2$) of the isopropyl groups of complexes **6** and **7**, clearly within the aromatic deshielding region, were also unexpectedly downfield.

The IR spectrometric measurement of CO stretching frequencies of metal carbonyl compounds is a well-known method of establishing the relative electrophilicity of a metal center. This technique was recently employed to measure electronic effects in the study of a Pt(II) system for C−H activation,[22] which screened several *N*-aryl α-diimine ligands spanning a similar σ range as in our study. Reaction of carbon monoxide to solutions of **1**−**7** and sodium tetrakis(3,5-bis(trifluoromethyl)phenyl)borate (NaBAF) afforded the desired [Pd(α-diimine)carbonylmethyl]$^+$BAF$^-$ salts **28**−**34** (Scheme 6). NMR and IR characterizations confirmed the structure of the carbonyl complexes by the existence of the Pd-*Me* group shifted slightly downfield in ^{1}H NMR compared to complexes **1**−**7**, the presence of BAF$^-$ signals in the ^{1}H and ^{13}C NMR, and the clearly visible CO IR stretching band from 2129 to 2140 cm^{-1}. The possibility of methyl migration to form an acyl complex was ruled out by the absence of an acyl carbonyl resonance in ^{13}C NMR, the lack of an acyl methyl signal in the ^{1}H NMR, and the presence of a CO ligand signal in the ^{13}C NMR.

The electron-donating ligands led to red-shifted CO stretching frequencies, in accordance with a more electron-rich metal capable of stronger M → CO π donation. The range in ν_{CO} for complexes **28**−**34**, about 10 cm^{-1}, is similar to the range reported for the Pt(II)-α-diimine system.[22] When the stretching frequencies were plotted versus the Hammet constant (σ), as shown in Figure 2, a linear correlation was obtained. Despite the large dihedral angle between the aryl rings and the α-diimine backbone,[3] the substituents are still able to significantly influence the electronic properties of the ligands and complexes. The quality of the correlation between the CO stretching frequency and substituent constant confirms that the Hammet constants can be used to quantitatively represent electronic effects in this system of Pd(II) complexes.

B. Ethylene Polymerization Studies Using the Pd(II)-α-Diimine Catalysts. Polyethylene Molecular Weight (MW). In this study a direct in situ activation of the methyl chlorides **1**−**7** was used.[35] To initiate polymerization, complexes **1**−**7** were activated in the presence of ethylene by the addition of excess NaBAF. The molecular weight of polyethylene obtained by catalysts **1**−**7** under 1 atm ethylene pressure and room temperature was measured by multiangle light scattering (MALS) analysis (Table 1). Catalyst **6** is omitted since it gave unusually low activities and low molecular weight (MW) polymer, which we attribute to the previously mentioned inability to completely purify the ligand. The polymerizations were run at relatively long time to ensure the polymers achieved the maximum molecular weights. A significant dependence on substituent was seen in the data, with an overall trend of higher MW polymer produced from catalysts bearing more electronic-donating ligands. The dependence of polymerization rate (turnover frequency, TOF) on substituent follows a similar trend. It should be noted that these observed trends might be partially complicated by the catalyst stability. It was generally observed that the more electron-deficient catalysts are less thermally stable. Conversely, the more electron-rich catalysts are more thermally stable and tend to afford higher polymerization productivities. The polymer MW is the result of complex interplay of monomer insertion, chain transfer, and potential catalyst decomposition. For a stable catalyst, the polymer MW is primarily controlled by the relative rates of monomer insertion and chain transfer (k_{ins}/k_{CT}). The similar trend in the dependence of MW and polymerization rate on ligand substituent suggests that the influence of ligand electronics on MW is primarily through the effect on insertion rate, k_{ins}. A more electron-donating ligand may better stabilize the transition state for monomer insertion than for chain transfer, resulting in a more productive catalyst that produces higher MW.

Polyethylene Branching Topology. The branching density (*B*) is rather constant for the polyethylenes made with different catalysts (Table 1). Our previous

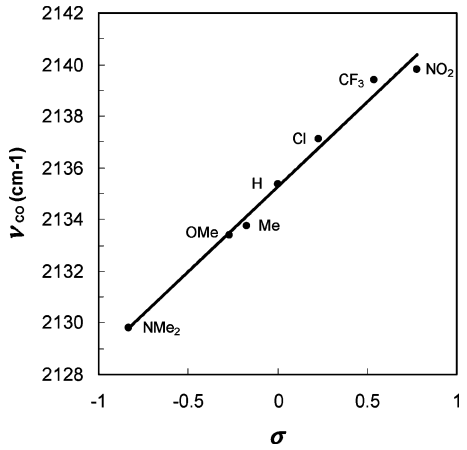

Figure 2. Plot of carbonyl ligand stretching frequencies versus Hammett substituent constant for complexes **28**–**34**.

Table 1. Ethylene Polymerization Data[a]

entry	catalyst	σ	B[b]	M_n[c]	M_w/M_n[d]	TON[e]	TOF[f]
1	**1**	0.78	100	133	1.81	280	16
2	**2**	0.54	95	286	1.44	8800	420
3	**3**	0.23	98	307	1.41	11 000	540
4	**4**	0	95	358	1.42	30 000	1700
5	**5**	-0.17	94	271	1.40	12 000	580
6	**7**	-0.83	95	462	1.36	23 000	1300

[a] Polymerization conditions: 1.0 atm ethylene, 25 °C, 20 h, 10.0 μmol catalyst, 2 equiv NaBAF, 40 mL CH_2Cl_2. [b] B = branches per 1000 carbon. [c] M_n = number-averaged MW in kg/mol, M_w = weight-averaged MW in kg/mol. [d] Polydispersity index. [e] TON = turnover number (moles of ethylene polymerized per mole of catalyst). [f] TOF = turnover frequency (TON per hour).

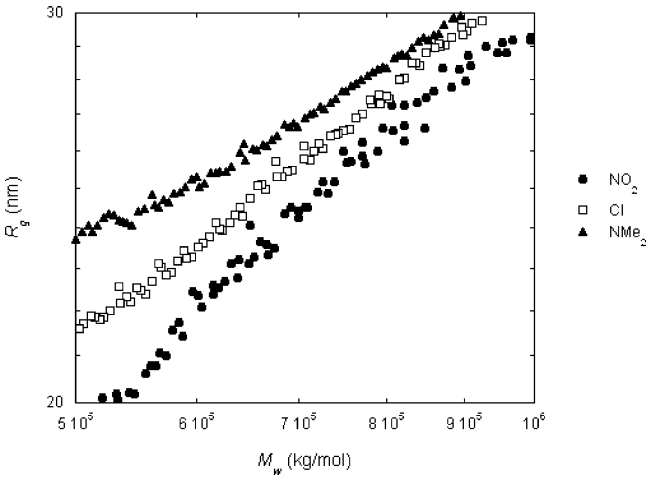

Figure 3. Logarithmetic plot of R_g versus M_n for polyethylenes made by catalysts **1**, **3**, and **7**, at 25 °C under general conditions and 20 h reaction times.

studies have shown that while the overall branching density B is relatively independent of reaction conditions,[4–6] the topology varies significantly with olefin concentration (or pressure), ranging from relatively linear with short branches to hyperbranched and dendritic. To determine the polymer branching topology, multiangle light scattering coupled to size exclusion chromatography (SEC) was employed to analyze the polyethylenes.[6,7,10] A logarithmic plot of polymer radius of gyration (R_g) as a function of MW, or M_w specifically, is shown in Figure 3. Compared at constant MW, more dendritic polymers should have smaller molecular size as expressed by smaller R_g values.[6,7,10] A clear dependence of polymer branching topology on substituent can be seen from the data in Figure 3. At constant MW, the most electron-deficient catalyst **1** afforded polymer with appreciably smaller value of R_g than polymer made by the most electron-rich catalyst **7**. Given the relatively constant branching density, the change in molecular size at constant MW can only be accounted for by the change in polymer branching topology. Therefore, at exactly the same polymerization conditions, the polymers made by the more electron-deficient catalysts are more dendritic than those made by the electron-rich catalysts.

We propose that the change in polymer topology is due to the influence of catalyst electronic structure on the polymerization kinetics. As discussed previously for ethylene polymerization using the prototype Pd(II)-α-diimine catalyst **4**,[6–10] the polymer branching topology is controlled by the competition between ethylene insertion rate and chain walking rate. Because ethylene insertion and chain walking have zero- and inverse first-order dependence on ethylene concentration (or pressure), respectively,[34] changing ethylene pressure will alter the relative rates for the two events, which subsequently results in a change in polyethylene branching topology. At low ethylene pressure, the chain walking process becomes faster than the insertion process. After each ethylene insertion, the Pd(II) catalyst can walk randomly on the polymer chain and the next insertion can occur at a random site on the polymer. Fine mechanistic studies by Brookhart and co-workers have also shown that the Pd(II) catalyst can easily walk through a tertiary carbon center.[34] The random walk of catalyst followed by monomer insertion in a statistical manner leads to the formation of dendritic polymer topology at low monomer concentrations. [6–10]

In our current investigation with *fixed* polymerization conditions, the ligand electronic effects on the polymerization kinetics (rate constant, k) must account for the change of polymer topology. Our data suggest that the more electron-rich catalyst (**7**) leads to a higher $k_{ins}/k_{walking}$ ratio and, therefore, affords a more linear polymer. Conversely, the more electron-deficient catalyst (**1**) should have a lower $k_{ins}/k_{walking}$ ratio and affords a more dendritic polymer. Our proposal offered in the last section to explain the trend of MW could be used to rationalize these effects on polymer topology as well. A more electron-donating ligand may better stabilize the transition state for monomer insertion than for chain walking, which should result in a higher $k_{ins}/k_{walking}$ ratio and afford a more linear polymer. To the best of our knowledge, this is the first report of ligand electronic effects on polymer topology for olefin polymerization catalysts. This provides a fundamentally different approach (catalyst approach) to control polyolefin branching topology, which complements our previous strategy of controlling polymer topology by polymerization conditions.[6,10]

C. Copolymerization Studies with Methyl Acrylate Using the Pd(II)-α-Diimine Catalysts. Incorporation Ratio of Polar Monomer. Copolymerizations of ethylene with methyl acrylate (MA) were carried out by adding a known volume of MA to the polymerization mixture prior to catalyst activation. The reactions

Scheme 7

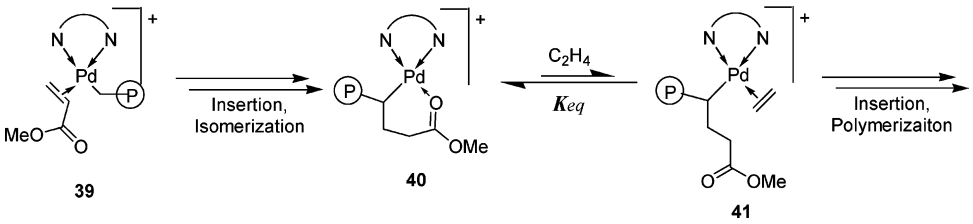

Table 2. Copolymerization Activities (TOF), Incorporation Ratios (*Ir*), and M_n for Copolymers at Varying Initial Concentrations of MA (in mol/L) under Copolymerization Conditions[a]

	TOF[b]				*Ir* (%)			M_n (kg/mol)		
catalyst	0[c]	0.12	0.58	1.67	0.12	0.58	1.67	0.12	0.58	1.67
1	220	10	0	0	0.1	–[d]	–	6.4	–	–
2	2000	40	<5	0	0.5	1.2	–	17	5.7	–
3	1800	130	30	<5	0.7	2.4	–	33	2.0	–
4	2600	130	10	<5	0.5	2.2	6.2	56	8.6	5.4
5	1600	160	50	20	0.7	2.6	4.9	62	15	0.56
6	920	170	30	< 5	0.6	2.9	6.1	41	12	4.7
7	2400	180	60	20	0.9	3.6	8.4	66	10	2.4

[a] Copolymerization conditions: general conditions followed for 6.5 h reaction times with an added 0.5, 2.5, or 8.0 mL of MA. [b] TOF values of "<5" means a trace of recovered polymer (0.01 g or less), while "0" indicates negligible polymer. [c] Ethylene homopolymerizations run for the same duration (6.5 h) shown for comparison. [d] Data not available.

were run at room temperature and 1 atm ethylene pressure. Data for copolymerizations are shown in Table 2. The incorporation ratio (*Ir*) was calculated from ^{1}H NMR analysis by the known method.[4] A strong dependence of *Ir* on substituent was observed for the catalysts. The catalysts bearing more electron-donating ligands exhibited significantly higher incorporation ratios than less electron-rich analogues. For example, for copolymerization at initial MA concentration of 0.12 M, the *Ir* increased from 0.1 to 0.9 mol % as the ligand substituent was changed from $-NO_2$ (**1**) to $-NMe_2$ (**7**). The trend was general over the three concentrations of MA examined, and deactivation of the catalysts was observed in the order **1**, **2**, **3**, then **4** as MA concentration increased. This trend has also been observed previously in two related α-diimine catalysts.[5] The olefin group of MA is a poorer σ-donor compared to ethylene. Presumably, decreasing the electrophilicity of the metal center increases the binding of the electron-deficient olefin (MA) relative to ethylene, which leads to an increase in the incorporation of MA.

Catalyst Tolerance to Polar Comonomer. We have observed significant differences in catalytic activity and polymer molecular weight obtained in copolymerizations using catalysts **1**−**7**, and the results are shown in Table 2. Both TON and TOF define the total monomer turnover and were calculated using an averaged monomer molecular weight based on the value of *Ir*. Electron-deficient catalysts were apparently "poisoned" at sufficient MA concentrations, affording a negligible amount of polymer. It has been shown that all Pd(II)-α-diimine catalysts exhibit a considerable decrease in activity in the presence of polar comonomers such as MA; however those bearing strongly electron-donating ligands were affected to a lesser degree. The existence of an ester chelate complex, such as **40**, following polymer insertion into MA has been proposed as a stable resting state, which is illustrated in Scheme 7.[5] Opening of the chelate by ethylene to give intermediate **41** is necessary for polymerization to continue, an unfavorable process, with measured K_{eq} values far less than unity.[5] The strength of chelation, and the resulting ease of chelate opening, should depend on the electron-donating ability of the ligand. An electrophilic Pd(II) should increase the strength of the Pd−O bond, manifested as increased metal oxophilicity.[36] The chelate intermediate is stabilized in complexes bearing electron-deficient ligands, leading to a decrease in K_{eq}. The greatly reduced activity of catalysts such as **1** occurred in conjunction with low molecular weights, likely the consequence of a low polymerization rate. Electron-rich metals of catalysts such as **7** have a decreased tendency to bind to electronegative groups, such as ester functionalities, making chelate opening more favorable and copolymerization faster overall.

Conclusions

A series of bis-(aryl)-α-diimine ligands having a range of electron-donating and -withdrawing substituents were successfully synthesized with the purpose to probe the ligand electronic effects on late transition metal olefin polymerization catalysts. The corresponding Pd(II)(α-diimine)MeCl complexes **1**−**7** and [Pd(II)(α-diimine)Me(CO)]$^+$BAF$^-$ complexes **28**−**34** were then prepared and characterized. NMR chemical shift analysis of complexes **1**−**7** and IR analysis of the CO stretching frequencies of the carbonyl complexes **28**−**34** confirmed that substitution does affect the electrophilicity of the metal center in a systematic manner. Complexes possessing ligands with donating substituents exhibited CO stretching bands that were shifted toward lower frequencies. The trend correlated well to the Hammet constant (σ) of the substituent.

Ethylene homopolymerizations and MA copolymerizations were carried out at room temperature and 1 atm of ethylene pressure using the series of complexes **1**−**7**. Electronic perturbations due to substitution on the α-diimine ligands were found to affect polymer properties such as molecular weight and branching topology. Overall, catalysts with electron-donating ligands were found to afford polymer with higher MW. It was observed for the first time that the ligand electronic structure of catalysts had a significant effect on topology of the polyethylene formed. More dendritic polyethylene was obtained with catalysts bearing more strongly electron-withdrawing ligands. More dramatic electronic effects were observed for ethylene copolymerization with MA using these catalysts. Electron-donating ligands led

(35) Schmid, M.; Eberhardt, R.; Klinga, M.; Leskela, M.; Rieger, B. *Organometallics* **2001**, *20*, 2321−2330.
(36) Crabtree, R. H. *The Organometallic Chemistry of the Transition Metals*; 3rd ed.; John Wiley and Sons: New York, 2001.

not only to higher incorporation ratios of MA in copolymers but also to a decreased degree of deactivation in the presence of MA. Higher catalytic activity toward copolymerization was observed in these more electron-rich catalysts, along with the production of higher MW copolymer.

Experimental Section

General Considerations. The catalyst handling was carried out in a Vacuum Atmospheres glovebox filled with nitrogen. All other moisture- and air-sensitive reactions were carried out in flame-dried glassware using magnetic stirring under a positive pressure of argon or nitrogen. Removal of organic solvents was accomplished by rotary evaporation and is referred to as concentrated in vacuo. Flash column chromatography was performed using forced flow on EM Science 230−400 mesh silica gel. NMR spectra were recorded on Bruker DRX400 and DRX500 FT-NMR instruments. Proton and carbon NMR spectra were recorded in ppm and were referenced to indicated solvents at indicated temperature, if different from ambient. Data were reported as follows: chemical shift, multiplicity (s = singlet, d = doublet, t = triplet, q = quartet), integration, and coupling constant(s) in hertz (Hz). Multiplets (m) were reported over the range (ppm) at which they appear at the indicated field strength. IR spectra were recorded on a Midac Prospect PRS-102 spectrometer. Elemental analysis (for new compounds) was preformed by Atlantic Microlab, Norcross, GA.

Materials. Toluene, tetrahydrofuran (THF), diethyl ether, and dichloromethane were purified by passing through solvent purification columns following the method introduced by Grubbs and are referred to as dry.[37] Unless otherwise stated, all other solvents and reagents were purchased from commercial suppliers and used as received. Anilines **8** and **9**,[25] unsubstituted ligand, and Pd complex **1**,[3,4] isopropenylboronic acid (**18**),[38] Pd(COD)MeCl,[39] and sodium tetrakis(3,5-bis(trifluoromethyl)phenyl)borate[40] (NaBAF) were prepared by known literature procedures. MA was uninhibited by passing through oven-dried basic alumina prior to use in polymerizations.

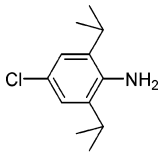

11

4-Chloro-2,6-diisopropylaniline (11).[26] To a solution of 10.0 mL (9.40 g, 53.0 mmol) of 2,6-diisopropylaniline (**10**) and 13.3 mL of 12.0 N HCl (159 mmol) in isobutanol (40 mL) was added 6.31 mL (55.7 mmol) of 30% aqueous H_2O_2. The mixture was stirred and heated at reflux for 20 h. The solvent was removed in vacuo, ethyl acetate was added (100 mL), and the solution was washed in water. After extracting twice more with ethyl acetate (50 mL) the organic fractions were combined and washed once with brine. The mixture was concentrated and separated by flash chromatography on silica with 6:1 hexanes/CH_2Cl_2 to give **10** as a reddish oil (7.46 g, 33%). NMR spectra were found to match a literature report.[41]

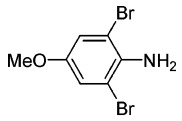

13

2,6-Dibromo-4-methoxyaniline (13).[28] To a solution of *p*-anisidine (2.00 g, 16.2 mmol) in 150 mL of CH_2Cl_2 and 50 mL of methanol were added 6.05 g of $CaCO_3$ (60.4 mmol) and 12.98 g of benzyltrimethylammonium tribromide (33.29 mmol). The resulting deep purple suspension was stirred for 2 h and then filtered. The filtrate was concentrated in vacuo and extracted into CH_2Cl_2 with dilute HCl added to break up emulsions. The organic phases were combined and washed with brine. The product was purified by flash chromatography through silica gel and with 1:1 hexanes/CH_2Cl_2 to afford **13** as a yellow-orange solid (3.10 g, 70%): ^{1}H NMR (500 MHz, $CDCl_3$) δ 3.72 (s, 3H), 4.19 (br s, 2H), 7.01 (s, 2H); ^{13}C NMR (125 MHz, $CDCl_3$) δ 56.6, 109.6, 118.5, 136.6, 152.5.

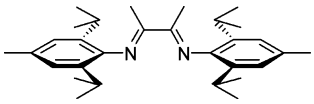

22

ArN=C(Me)−C(Me)=NAr, Ar ≡ 2,6-*i*Pr$_2$-4-MeC$_6$H$_2$-(^{Me}N∧N, 22).[27,30] A round-bottom flask was charged with 3.00 g (11.3 mmol) of 2,6-dibromo-4-methylaniline (**12**) and 150 mg of $PdCl_2$(dppf) and placed under high vacuum for 20 min. The flask was then filled with nitrogen and 40 mL of dry THF and then stirred at rt until all solid had dissolved. The flask was then cooled to −78 °C, and to this solution was transferred 90.6 mL (45.3 mmol) of a solution of isopropenylmagnesium bromide (0.5 M) in THF with stirring. Upon completion of addition, the mixture was allowed to warm to rt and then heated to reflux for 20 h. The mixture was cooled and carefully quenched with 50 mL of 2 M HCl. Aqueous NaOH was added until basic, and the mixture was extracted into diethyl ether. The organic layer was then washed with brine before being dried over Na_2SO_4 and concentrated. The crude oil (**14**) was dissolved in 30 mL of methanol and 250 mg of 10% by wt Pd/C was added. The mixture was stirred under hydrogen for 24 h. The catalyst was replaced by filtering through Celite, adding a new 250 mg quantity of Pd/C, and placed under a hydrogen atmosphere for another 24 h. The replacement procedure was repeated one last time before filtering after 3 days total reaction time. The mixture was concentrated in vacuo, extracted in diethyl ether, dried over Na_2SO_4, and concentrated again to give crude **16**. The concentrated oil was then dissolved in 30 mL of methanol, and to this solution were added two drops of formic acid and 295 μL of 2,3-butanedione (290 mg, 3.36 mmol). The solution was then heated to reflux and stirred for 3 days. The mixture was concentrated in vacuo, and the residue was recrystallized from methanol to give **22** as pale yellow-green crystals (260 mg). Flash chromatography of the concentrated mother liquor afforded an additional 142 mg of **22** (16%) and 324 mg of monocondensed byproduct: ^{1}H NMR (400 MHz, $CDCl_3$) δ 1.15 (d, 12H, J = 6.9 Hz), 1.17 (d, 12H, J = 7.0 Hz), 2.05 (s, 6H), 2.35 (s, 6H), 2.68 (septet, 4H, J = 6.9 Hz), 6.96 (s, 2H); ^{13}C NMR (100 MHz, $CDCl_3$) δ 16.5, 21.36, 22.7, 23.0, 28.4, 123.7, 132.7, 134.9, 143.7, 168.5. Anal. Calcd for $C_{30}H_{44}N_2$: C, 83.28; H, 10.25; N, 6.47. Found: C, 83.04; H, 10.30; N, 6.45.

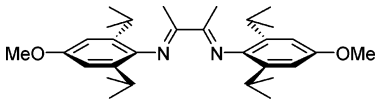

23

(37) Pangborn, A. B.; Giardello, M. A.; Grubbs, R. H.; Rosen, R. K.; Timmers, F. J. *Organometallics* **1996**, *15*, 1518−1520.
(38) Braun, J.; Normant, H. *Bull. Soc. Chim. Fr.* **1966**, 2557.
(39) Rulke, R. E.; Ernsting, J. M.; Spek, A. L.; Elsevier, C. J.; Vanleeuwen, P. W. N. M.; Vrieze, K. *Inorg. Chem.* **1993**, *32*, 5769−5778.
(40) Brookhart, M.; Grant, B.; Volpe, A. F. *Organometallics* **1992**, *11*, 3920−3922.
(41) Dombroski, M. A.; Eggler, J. F. (Pfizer Inc., USA) PCT Int. Appl. Wo, 1998; p 81.

ArN=C(Me)−C(Me)=NAr, Ar ≡ 2,6-*i*Pr$_2$-4-OMeC$_6$H$_2$ (^{OMe}N∧N, 23).[27,30] A round-bottom flask was charged with 3.51 g (12.5 mmol) of **13** and 150 mg of $PdCl_2$(dppf) and placed under high vacuum for 20 min. The flask was then filled with nitrogen and 40 mL of dry THF and then stirred at rt until all solid had dissolved. The flask was then cooled to −78 °C, and to this solution was transferred 100.0 mL (50.0 mmol) of a solution of isopropenylmagnesium bromide (0.5 M) in THF with stirring. Upon completion of addition, the mixture was allowed to warm to rt and then heated to reflux for 20 h. The mixture was cooled and carefully quenched with 50 mL of 2 M HCl. Aqueous NaOH was added until basic, and the mixture was extracted into diethyl ether. The organic layer was then washed with brine before being dried over Na_2SO_4 and concentrated. The crude oil (**15**) was dissolved in 30 mL of methanol, and 250 mg of 10% by wt Pd/C was added. The mixture was stirred under hydrogen for 24 h. The catalyst was replaced by filtering through Celite, adding a new 250 mg quantity of Pd/C, and placed under a hydrogen atmosphere for 24 h. The replacement procedure was repeated one last time before filtering after 3 days total reaction time. The mixture was concentrated in vacuo, extracted in diethyl ether, dried over Na_2SO_4, and concentrated again to give crude **17**. The concentrated oil was then dissolved in 20 mL of methanol, and to this solution were added two drops of formic acid and 172 μL of 2,3-butanedione (1.96 mmol), based on an estimated aniline purity of 80%. The solution was then heated to reflux and stirred for 3 days. The mixture was concentrated in vacuo, and the residue was recrystallized from methanol to give **23** as pale yellow-green crystals. NMR analysis indicated the existence of an impurity that was not removed by additional recrystallization attempts (192 mg, 19%): ^{1}H NMR (500 MHz, $CDCl_3$) δ 1.16 (d, 12H, J = 6.9 Hz), 1.17 (d, 12H, J = 7.0 Hz), 2.05 (s, 6H), 2.70 (septet, 4H, J = 6.9 Hz), 3.83 (s, 6H), 6.96 (s, 2H); ^{13}C NMR (125 MHz, $CDCl_3$) δ 16.6, 22.67, 22.95, 28.7, 55.3, 108.6, 136.6, 139.8, 156.3, 169.3. Anal. Calcd for $C_{30}H_{44}N_2O_2$: C, 77.54; H, 9.54; N, 6.03. Found: C, 76.82; H, 9.48; N, 6.04.

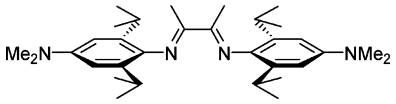

24

ArN=C(Me)−C(Me)=NAr, Ar ≡ 2,6-*i*Pr$_2$-4-NMe$_2$C$_6$H$_2$ (^{NMe2}N∧N, 24).[30] To a solution of **9** (6.69 g, 30.4 mmol) in methanol (20 mL) was added 1.07 mL (1.05 g, 12.1 mmol) of 2,3-butanedione and five drops of formic acid. The mixture was heated to reflux for 3.5 h with stirring. The solution was concentrated in vacuo, and the residue was washed with methanol (2 × 20 mL) and filtered. The resulting solid was recrystallized in methanol to afford **24** as a bright orange solid (3.142 g, 21%): ^{1}H NMR (500 MHz, $CDCl_3$) δ 1.17 (d, 12H, J = 6.7 Hz), 1.18 (d, 12H, J = 6.8 Hz), 2.06 (s, 6H), 2.72 (septet, 4H, J = 6.9 Hz), 2.95 (s, 12H), 6.62 (s, 4H); ^{13}C NMR (125 MHz, $CDCl_3$) δ 17.1, 23.2, 23.5, 41.9, 109.0, 136.4, 138.3, 148.1, 169.7. Anal. Calcd for $C_{32}H_{50}N_4$: C, 78.31; H, 10.27; N, 11.42. Found: C, 78.55; H; 10.36; N, 11.34.

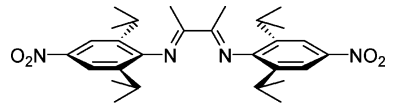

25

ArN=C(Me)−C(Me)=NAr, Ar ≡ 2,6-*i*Pr$_2$-4-NO$_2$C$_6$H$_2$ (^{NO2}N∧N, 25). To a solution of **8** (9.187 g, 41.33 mmol) in 120 mL of benzene was added 1.63 mL of 2,3-butanedione (1.61 g, 18.7 mmol) followed by 200 mg of 10-camphorsulfonic acid. The flask was then fitted with a medium Soxhlet extractor with condenser, and the extractor was filled halfway with oven-dried 5 Å molecular sieves. The mixture was heated to reflux and stirred for 2 days. The mixture was concentrated in vacuo, and diethyl ether (20 mL) was added. The resultant slurry was filtered and washed again with diethyl ether and dried to afford ligand **25** as a yellow-green solid (4.516 g, 49%): ^{1}H NMR (500 MHz, CD_2Cl_2) δ 1.20 (d, 12H, J = 6.8 Hz), 1.27 (d, 12H, J = 6.9 Hz), 2.09 (s, 6H), 2.73 (septet, 4H, J = 6.9 Hz), 8.07 (s, 4H); ^{13}C NMR (125 MHz, $CDCl_3$) δ 17.5, 22.7, 23.1, 119.8, 136.9, 145.3, 152.1, 168.3. Anal. Calcd for $C_{28}H_{38}N_4O_4$: C, 67.99; H, 7.74; N, 11.33. Found: C, 67.52; H, 7.79; N, 10.81.

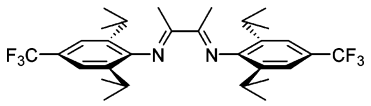

26

ArN=C(Me)−C(Me)=NAr, Ar ≡ 2,6-*i*Pr$_2$-4-CF$_3$C$_6$H$_2$ (^{CF3}N∧N, 26).[29] A round-bottom flask was charged with 2.60 g (8.15 mmol) of 2,6-dibromo-4-(trifluoromethyl)aniline (**19**) and 500 mg of $Pd(PPh_3)_4$ (5.3 mol %) and placed under high vacuum for 20 min. The flask was filled with argon and 100 mL of 1,4-dioxane. To this solution was transferred a solution of 2.10 g of **18** (24.5 mmol) in 30 mL of ethanol and 25 mL of 2 M aqueous K_2CO_3. The mixture was heated to reflux with stirring for 24 h, filtered through a Celite and silica plug, and extracted into diethyl ether. The organic layer was dried over Na_2SO_4 and concentrated to give a pale greenish oil. The crude oil (**20**) was dissolved in 30 mL of methanol, and 250 mg of 10% by wt Pd/C was added. The mixture was stirred under hydrogen for 24 h. The catalyst was replaced by filtering through Celite, adding a new 250 mg quantity of Pd/C, and placed under a hydrogen atmosphere for 24 h. The replacement procedure was repeated one last time before filtering after 3 days total reaction time. The mixture was concentrated in vacuo, extracted in diethyl ether, dried over Na_2SO_4, and concentrated again to give crude **21**. The concentrated mixture yielded 1.72 g of brownish oil that was dissolved in 120 mL of benzene. To this solution were added 50 mg of 10-CSA and 232 μL of 2,3-butanedione (227 mg, 2.64 mmol), based on an estimated aniline purity of 80%. The flask was then fitted with a medium Soxhlet extractor which was filled halfway with oven-dried 5 Å molecular sieves. The mixture was heated to reflux and stirred for 3 days. The mixture was concentrated in vacuo, and the residue was recrystallized from methanol to give **26** as pale yellow crystals (425 mg). Further condensation of the recovered mother liquor by adding an additional 161 μL of 2,3-butanedione afforded 381 mg of **26** after 3 days to give a total yield of 26%: ^{1}H NMR (500 MHz, $CDCl_3$) δ 1.18 (d, 12H, J = 6.9 Hz), 1.23 (d, 12H, J = 6.9 Hz), 2.07 (s, 6H), 2.71 (septet, 4H, J = 6.9 Hz), 7.40 (s, 2H); ^{13}C NMR (125 MHz, $CDCl_3$) δ 16.7, 22.36, 22.73, 28.7, 120.3, 125.9, 126.2, 135.7, 148.9, 168.2. Anal. Calcd for $C_{30}H_{38}N_2F_6$: C, 66.65; H, 7.08; N, 5.18. Found: C, 66.53; H, 7.11; N, 5.10.

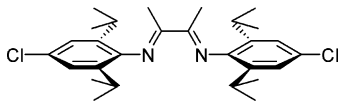

27

ArN=C(Me)−C(Me)=NAr, Ar ≡ 2,6-*i*Pr$_2$-4-ClC$_6$H$_2$ (^{Cl}N∧N, 27). To a solution of **11** (1.72 g, 8.12 mmol) in 120 mL of benzene was added 321 μL of 2,3-butanedione (315 mg, 3.65 mmol) followed by 150 mg of 10-camphorsulfonic acid. The flask was then fitted with a medium Soxhlet extractor which was filled halfway with oven-dried 5 Å molecular sieves. The mixture was heated to reflux and stirred for 2 days. The mixture was concentrated in vacuo, and the residue was recrystallized from ethanol to give **27** as pale yellow crystals (0.981 g, 51%): ^{1}H NMR (400 MHz, $CDCl_3$) δ 1.15 (d, 12H, J = 6.9), 1.17 (d, 12H, J = 6.9 Hz), 2.04 (s, 6H), 2.65 (septet,

4H, J = 6.9 Hz), 7.12 (s, 4H); ^{13}C NMR (100 MHz, $CDCl_3$) δ 16.5, 22.35, 22.68, 28.6, 123.2, 129.1, 137.0, 144.4, 168.7. Anal. Calcd for $C_{28}H_{38}N_2Cl_2$: C, 71.02; H, 8.09; N, 5.92. Found: C, 71.08; H, 8.11; N, 5.86.

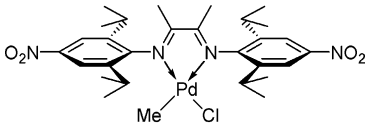

1

(^{NO2}N∧N)PdMeCl (1).[32] To a −35 °C solution of $(PhCN)_2PdCl_2$ (513 mg, 1.34 mmol) in 5.0 mL of dry CH_2Cl_2 was added 454 μL (598 mg, 3.34 mmol) of tetramethyltin under argon. This mixture was stirred at −35 °C for 2.5 h, after which a solution of ligand **25** (551 mg, 1.114 mmol) in 3.0 mL of dry CH_2Cl_2 was added. The reaction mixture was kept at low temperature for 15 min then warmed to rt. The mixture was stirred overnight and then placed directly on a silica gel column for purification by flash chromatography with 5:4:1 hexanes/CH_2Cl_2/EtOAc as the mobile phase. The orange fraction was concentrated and dried in vacuo overnight to give **1** as an orange solid (533 mg, 74%): ^{1}H NMR (500 MHz, $CDCl_3$) δ 0.55 (s, 3H), 1.23 (d, 6H, J = 7.8 Hz), 1.25 (d, 6H, J = 7.3 Hz), 1.42 (d, 6H, J = 6.8 Hz), 1.48 (d, 6H, J = 6.7 Hz), 2.09 (s, 3H), 2.13 (s, 3H), 3.05 (septet, 2H, J = 6.9 Hz), 3.09 (sep, 2H, J = 6.9 Hz), 8.14 (s, 2H), 8.19 (s, 2H); ^{13}C NMR (125 MHz, $CDCl_3$) δ 4.5, 20.6, 21.9, 23.3, 23.7, 23.9, 24.0, 29.6, 30.0, 119.9, 120.5, 140.5, 141.3, 146.8, 147.0, 147.5, 147.9, 169.9, 174.7. Combustion (C, H, N): Anal. Calcd for $C_{29}H_{41}PdN_4O_4Cl$: C, 53.46; H, 6.34; N, 8.60. Found: C, 53.45; H, 6.49; N, 8.28. LRMS (ES/MS, *m/z* in MeCN): Anal. Calcd for $C_{29}H_{41}PdN_4O_4Cl$: 656 (M − Cl^- + MeCN). Found: 656.

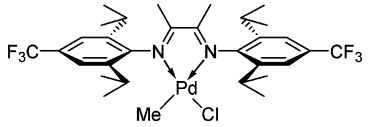

2

(^{CF3}N∧N)PdMeCl (2).[32] To a −35 °C solution of $(PhCN)_2PdCl_2$ (255 mg, 0.666 mmol) in 5.0 mL of dry CH_2Cl_2 was added 241 μL (318 mg, 3.20 mmol) of tetramethyltin under argon. After stirring at −35 °C for 2.5 h a solution of ligand **26** (300 mg, 0.549 mmol) in 2.0 mL of dry CH_2Cl_2 was added. The reaction mixture was warmed to rt and stirred overnight, then placed directly on a silica gel column for purification by flash chromatography and eluted with 5:4:1 hexanes/CH_2Cl_2/EtOAc. The orange fraction was concentrated and dried in vacuo overnight to give **2** as an orange solid (312 mg, 81%): ^{1}H NMR (500 MHz, $CDCl_3$) δ 0.50 (s, 3H), 1.19 (t, 12H, J = 6.9 Hz), 1.37 (d, 6H, J = 6.8 Hz), 1.43 (d, 6H, J = 6.8 Hz), 2.05 (s, 3H), 2.07 (s, 3H), 3.05 (septet, 2H, J = 6.9 Hz), 3.08 (septet, 2H, J = 6.9 Hz), 7.46 (s, 2H), 7.53 (s, 2H); ^{13}C NMR (125 MHz, $CDCl_3$) δ 3.5, 20.2, 21.6, 23.12, 23.41, 23.71, 23.78, 28.9, 29.4, 120.8, 121.5, 123.04, 123.37, 125.20, 125.53, 129.18, 129.43, 130.13, 130.39, 139.19, 139.94, 144.40, 144.51, 170.0, 174.6. Combustion (C, H, N): Anal. Calcd for $C_{31}H_{41}PdN_2ClF_6$: C, 53.38; H, 5.92; N, 4.02. Found: C, 53.50; H, 6.10; N, 3.92. LRMS (ES/MS, *m/z* in MeCN): Anal. Calcd for $C_{31}H_{41}PdN_2ClF_6$: 702 (M − Cl^- + MeCN). Found: 702.

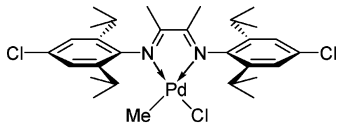

3

(^{Cl}N∧N)PdMeCl (3).[31] To a solution of ligand **27** (400 mg, 0.845 mmol) in dry CH_2Cl_2 (20 mL) was added 213 mg (0.807 mmol) of Pd(COD)MeCl. After stirring the mixture for 2 days at room temperature, it was concentrated in vacuo to give a red-orange residue that was washed with hexanes (2 × 5 mL). The remaining solid was then dried in vacuo for 2 days to yield the complex **3** as an orange solid (476 mg, 89%): ^{1}H NMR (500 MHz, $CDCl_3$) δ 0.53 (s, 3H), 1.16 (t, 12H, J = 6.9 Hz), 1.34 (d, 6H, J = 6.8 Hz), 1.41 (d, 6H, J = 6.8 Hz), 2.04 (s, 3H), 2.06 (s, 3H), 3.00 (septet, 2H, J = 6.9 Hz), 3.02 (septet, 2H, J = 6.9 Hz), 7.19 (s, 2H), 7.24 (s, 2H); ^{13}C NMR (125 MHz, $CDCl_3$) δ 3.4, 19.8, 21.2, 22.96, 23.22, 23.54, 23.59, 28.8, 29.2, 123.9, 124.5, 132.7, 133.5, 139.93, 140.01, 140.04, 140.60, 169.8, 174.4. Combustion (C, H, N): Anal. Calcd for $C_{29}H_{41}PdN_2Cl_3$: C, 55.25; H, 6.56; N, 4.44. Found: C, 54.66; H, 6.48; N, 4.08. LRMS (ES/MS, *m/z* in MeCN): Anal. Calcd for $C_{29}H_{41}PdN_2Cl_3$: 634 (M − Cl^- + MeCN). Found: 634.

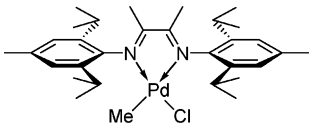

5

(^{Me}N∧N)PdMeCl (5).[31] To a solution of ligand **22** (245 mg, 0.566 mmol) in dry CH_2Cl_2 (20 mL) was added 140 mg (0.528 mmol) of Pd(COD)MeCl. After stirring the mixture for 18 h at room temperature, it was concentrated in vacuo to give a dark brown residue, which was washed with hexanes (2 × 5 mL). The remaining solid was then dried in vacuo for 2 days to yield the complex **5** as an orange solid (284 mg, 85%): ^{1}H NMR (500 MHz, $CDCl_3$) δ 0.52 (s, 3H), 1.15 (dd, 12H, J = 6.9 Hz, 1.9 Hz), 1.33 (d, 6H, J = 6.9 Hz), 1.41 (d, 6H, J = 6.9 Hz), 2.02 (s, 3H), 2.04 (s, 3H), 2.34 (s, 3H), 2.37 (s, 3H), 3.02 (septet, 4H, J = 6.7 Hz), 7.01 (s, 2H), 7.05 (s, 2H); ^{13}C NMR (125 MHz, $CDCl_3$) δ 3.4, 20.0, 21.48, 21.89, 22.04, 23.61, 23.87, 24.2, 28.8, 29.3, 124.5, 125.0, 136.6, 137.5, 138.0, 138.7, 169.7, 174.3. Combustion (C, H, N): Anal. Calcd for $C_{31}H_{47}PdN_2Cl$: C, 63.15; H, 8.03; N, 4.75. Found: C, 63.03; H, 7.93; N, 4.74. LRMS (ES/MS, *m/z* in MeCN): Anal. Calcd for $C_{31}H_{47}PdN_2Cl$: 594 (M − Cl^- + MeCN). Found: 594.

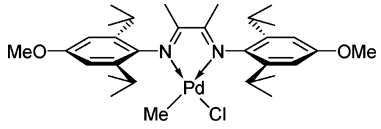

6

(^{OMe}N∧N)PdMeCl (6).[31] To a solution of ligand **23** (150 mg, 0.323 mmol) in dry CH_2Cl_2 (20 mL) was added 81 mg (0.31 mmol) of Pd(COD)MeCl. After stirring the mixture for 26 h at room temperature, it was concentrated in vacuo to give a dark red-orange residue, which was washed with hexanes (2 × 5 mL). The remaining oil was then dried in vacuo overnight. The residue was dissolved in dry CH_2Cl_2 (1 mL) and precipitated from hexanes (5 mL) and dried once again to yield the complex **6** as a red-orange solid (284 mg, 85%, 90% estimated purity). An attempt at purification by flash chromatography through silica gel as for **1** and **2** was not successful: ^{1}H NMR (400 MHz, $CDCl_3$) δ 0.53 (s, 3H), 1.12 (dd, 12H, J = 6.9 Hz, 1.9 Hz), 1.28 (d, 6H, J = 6.9 Hz), 1.42 (d, 6H, J = 6.9 Hz), 2.02 (s, 3H), 2.04 (s, 3H), 3.04 (septet, 2H, J = 6.7 Hz), 3.06 (septet, 2H, J = 6.7 Hz), 3.83 (s, 3H), 3.85 (s, 3H), 6.76 (s, 2H), 6.78 (s, 2H); ^{13}C NMR (100 MHz, $CDCl_3$) δ 2.8, 19.5, 21.0, 23.00, 23.19, 23.42, 23.58, 28.6, 29.1, 54.9, 55.2, 108.6, 109.1, 135.16, 135.20, 139.30, 139.97, 158.17, 158.65, 169.8, 174.5. LRMS (ES/MS, *m/z* in MeCN): Anal. Calcd for $C_{31}H_{47}PdN_2O_2Cl$: 626 (M − Cl^- + MeCN). Found: 626.

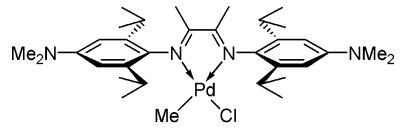

7

(^{NMe2}N∧N)PdMeCl (7).[31] To a solution of ligand **24** (805.6 mg, 1.64 mmol) in dry CH_2Cl_2 (20 mL) was added 414 mg (1.56 mmol) of Pd(COD)MeCl. After stirring the mixture overnight at room temperature, it was concentrated in vacuo to give a dark brown residue, which was washed with hexanes (3 × 10 mL). The remaining solid was then dried in vacuo for 2 days to yield the complex **7** as a dark brown solid (885 mg, 84%): ^{1}H NMR (400 MHz, $CDCl_3$) δ 0.53 (s, 3H), 1.15 (d, 6H, J = 6.9 Hz), 1.16 (d, 6H, J = 6.9 Hz), 1.34 (d, 6H, J = 6.8 Hz), 1.42 (d, 6H, J = 6.8 Hz), 2.01 (s, 3H), 2.03 (s, 3H), 2.98 (s, 6H), 2.99 (s, 6H), 3.05−3.09 (m, 2H), 6.57 (s, 2H), 6.58 (s, 2H); ^{13}C NMR (100 MHz, $CDCl_3$) δ 2.8, 19.5, 20.9, 23.1, 23.3, 23.7, 28.5, 29.1, 40.6, 40.7, 107.3, 107.5, 132.6, 138.7, 139.2, 149.5, 169.7, 174.4. Combustion (C, H, N): Anal. Calcd for $C_{33}H_{53}PdN_4Cl$: C, 61.20; H, 8.25; N, 8.65. Found: C, 60.13; H, 8.11; N, 8.65. LRMS (ES/MS, *m/z* in MeCN): Anal. Calcd for $C_{33}H_{53}PdN_4Cl$: 652 (M − Cl^- + MeCN). Found: 652.

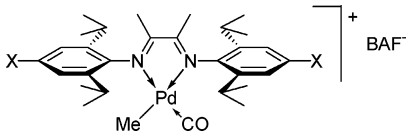

General Procedure for [Pd(diimine)Me(CO)]BAF Formation. To an oven-dried vial charged with 35.0 μmol of one of complexes **1**−**7** and NaBAF (1.0 equiv) was added 5.0 mL of dry CH_2Cl_2 under an atmosphere of CO. The solution was stirred for 10 min under constant addition of CO, leading to a darkening and an increase in turbidity of the solution. The mixture was filtered through Celite and concentrated in vacuo to afford the complexes **28**−**34**, respectively, as yellow to deep blue solids. Spectral data for the BAF counterion can be found elsewhere and will not be repeated in the spectroscopic data listed below for the cationic carbonyl complexes of **28**−**34**.[5]

[(^{NO2}N∧N)PdMe(CO)]$^+$, 28: ^{1}H NMR (500 MHz, CD_2Cl_2) δ 0.94 (s, 3H, Pd-*Me*), 1.29 (d, 6H, J = 6.8 Hz), 1.34 (d, 6H, J = 6.8 Hz), 1.38 (d, 6H, J = 6.8 Hz), 1.45 (d, 6H, J = 6.8 Hz), 2.34 (s, 3H), 2.45 (s, 3H), 2.72 (septet, 2H, J = 6.9 Hz), 2.87 (septet, 2H, J = 6.8 Hz), 8,29 (s, 4H); ^{13}C NMR (125 MHz, CD_2Cl_2) δ 11.3 (Pd-*Me*), 21.0, 22.96, 23.02, 23.26, 23.57, 30.36, 119.7, 121.31, 121.36, 139.6, 141.3, 142.5, 146.6, 148.97, 149.28, 173.1 (CO), 177.0, 184.2; IR (CH_2Cl_2) 2139.8 cm^{-1} [ν(CO)].

[(^{CF3}N∧N)PdMe(CO)]$^+$, 29: ^{1}H NMR (500 MHz, CD_2Cl_2) δ 0.91 (s, 3H, Pd-*Me*), 1.25 (d, 6H, J = 6.8 Hz), 1.30 (d, 6H, J = 6.9 Hz), 1.34 (d, 6H, J = 6.9 Hz), 1.42 (d, 6H, J = 6.8 Hz), 2.31 (s, 3H), 2.42 (s, 3H), 2.71 (septet, 2H, J = 6.9 Hz), 2.86 (septet, 2H, J = 6.8 Hz), 7.68 (s, 2H), 7.69 (s, 2H); ^{13}C NMR (125 MHz, CD_2Cl_2) δ 10.8 (Pd-*Me*), 20.7, 22.82, 22.98, 23.29, 23.58, 30.08, 30.11, 122.90, 122.93, 138.5, 139.3, 140.15, 140.75, 173.4 (CO), 176.8, 184.1; IR (CH_2Cl_2) 2139.4 cm^{-1} [ν(CO)].

[(^{Cl}N∧N)PdMe(CO)]$^+$, 30: ^{1}H NMR (500 MHz, CD_2Cl_2) δ 0.90 (s, 3H, Pd-*Me*), 1.21 (d, 6H, J = 6.8 Hz), 1.25 (d, 6H, J = 6.9 Hz), 1.30 (d, 6H, J = 6.8 Hz), 1.37 (d, 6H, J = 6.9 Hz), 2.29 (s, 3H), 2.40 (s, 3H), 2.63 (septet, 2H, J = 6.8 Hz), 2.78 (septet, 2H, J = 6.9 Hz), 7.38 (s, 2H), 7.39 (s, 2H); ^{13}C NMR (125 MHz, CD_2Cl_2) δ 10.5 (Pd-*Me*), 20.5, 22.7, 23.01, 23.31, 23.58, 29.99, 30.05, 125.5, 126.00, 126.06, 135.9, 136.34, 136.53, 139.2, 140.8, 173.6 (CO), 176.9, 184.3; IR (CH_2Cl_2) 2137.1 cm^{-1} [ν(CO)].

[(^{H}N∧N)PdMe(CO)]$^+$, 31: ^{1}H NMR (500 MHz, CD_2Cl_2) δ 0.85 (s, 3H, Pd-*Me*), 1.22 (d, 6H, J = 6.8 Hz), 1.27 (d, 6H, J = 6.8 Hz), 1.31 (d, 6H, J = 6.8 Hz), 1.38 (d, 6H, J = 6.8 Hz), 2.28 (s, 3H), 2.39 (s, 3H), 2.67 (septet, 2H, J = 6.9 Hz), 2.83 (septet, 2H, J = 6.8 Hz), 7.38−7.49 (m, 6H); ^{13}C NMR (125 MHz, $CDCl_3$) δ 9.9 (Pd-*Me*), 20.0, 22.2, 23.30, 23.55, 23.80, 23.87, 29.83, 29.90, 125.5, 130.10, 130.54, 136.8, 138.02, 138.48, 142.6, 173.8 (CO), 175.8, 183.3; IR (CH_2Cl_2) 2135.4 cm^{-1} [ν(CO)].

[(^{Me}N∧N)PdMe(CO)]$^+$, 32: ^{1}H NMR (500 MHz, CD_2Cl_2) δ 0.84 (s, 3H, Pd-*Me*), 1.19 (d, 6H, J = 6.9 Hz), 1.24 (d, 6H, J = 6.9 Hz), 1.29 (d, 6H, J = 6.8 Hz), 1.36 (d, 6H, J = 6.8 Hz), 2.25 (s, 3H), 2.36 (s, 3H), 2.40 (s, 6H), 2.62 (septet, 2H, J = 6.8 Hz), 2.80 (septet, 2H, J = 6.9 Hz), 7.17 (s, 2H), 7.18 (s, 2H); ^{13}C NMR (125 MHz, CD_2Cl_2) δ 9.7 (Pd-*Me*), 20.2, 21.43, 21.47, 22.4, 23.18, 23.52, 23.72, 23.77, 29.66, 29.75, 125.95, 126.06, 136.7, 139.8, 140.28, 140.47, 174.1 (CO), 176.2, 183.7; IR (CH_2Cl_2) 2133.7 cm^{-1} [ν(CO)].

[(^{OMe}N∧N)PdMe(CO)]$^+$, 33: ^{1}H NMR (500 MHz, CD_2Cl_2) δ 0.85 (s, 3H, Pd-*Me*), 1.20 (d, 6H, J = 6.8 Hz), 1.25 (d, 6H, J = 6.8 Hz), 1.29 (d, 6H, J = 6.8 Hz), 1.37 (d, 6H, J = 6.8 Hz), 2.26 (s, 3H), 2.37 (s, 3H), 2.64 (septet, 2H, J = 6.8 Hz), 2.82 (septet, 2H, J = 6.9 Hz), 3.85 (s, 3H), 3.86 (s, 3H), 6.87 (s, 2H), 6.88 (s, 2H); ^{13}C NMR (125 MHz, CD_2Cl_2) δ 9.9 (Pd-*Me*), 20.3, 22.4, 23.15, 23.46, 23.66, 23.69, 29.99, 30.08, 55.8, 110.6, 125.5, 131.5, 136.3, 138.8, 140.4, 160.59, 160.82, 174.0 (CO), 176.8, 184.3; IR (CH_2Cl_2) 2133.4 cm^{-1} [ν(CO)].

[(^{NMe2}N∧N)PdMe(CO)]$^+$, 34: ^{1}H NMR (500 MHz, CD_2Cl_2) δ 0.84 (s, 3H, Pd-*Me*), 1.19 (d, 6H, J = 6.9 Hz), 1.24 (d, 6H, J = 6.9 Hz), 1.29 (d, 6H, J = 6.8 Hz), 1.36 (d, 6H, J = 6.8 Hz), 2.25 (s, 3H), 2.35 (s, 3H), 2.66 (septet, 2H, J = 6.9 Hz), 2.85 (septet, 2H, J = 6.8 Hz), 3.02 (s, 12H), 6.60 (s, 2H), 6.61 (s, 2H); ^{13}C NMR (125 MHz, CD_2Cl_2) δ 9.6 (Pd-*Me*), 20.1, 22.2, 23.25, 23.55, 23.69, 23.76, 29.96, 30.12, 40.52, 40.55, 107.96, 108.07, 128.5, 133.6, 138.1, 139.6, 151.25, 151.39, 174.3 (CO), 176.3, 184.1; IR (CH_2Cl_2) 2129.8 cm^{-1} [ν(CO)].

General in-Situ-Activated Polymerization Procedure. An evacuated oven-dried 100 mL two- or three-neck flask fitted with a septum and ethylene feed was charged with 40 mL of dry toluene. Temperature was controlled by placement in an external bath as needed. Ethylene was added to fill the vacuum and slowly ran through the flask and out the bubbler to maintain ambient pressure. After 20 min with rapid stirring, 2.0 mL of a 0.0050 M solution (10.0 μmol) of complexes **1**−**7** in dry CH_2Cl_2 and 3.0 mL of NaBAF slurry (2 equiv) in dry CH_2Cl_2 were then added to the mixture. The mixture was allowed to stir at a given temperature for an allotted time period, depending on experiment. Upon quenching with triethylsilane (0.5 mL),[42] the solution was filtered through a Celite and silica gel plug and concentrated in vacuo. Cold methanol (40 mL) was then added, and the mixture was chilled for 30 min at −35 °C. The suspensions were then decanted and placed under soft vacuum overnight with heating (70 °C) to dry the polymer.

Molecular Weight and Topology Experiments. The above procedure for in-situ-activated polymerizations was followed using an external bath set at 25 °C. Reactions were run for 20 h and worked up in the manner described in the general procedure. Polymer samples were collected and characterized by SEC-MALS as described below.

Copolymerizations with Methyl Acrylate. The above procedure for in-situ-activated polymerizations was followed using an external bath set at 25 °C, except a known volume (either 0.5, 2.5, or 8.0 mL) of MA was added prior to catalyst activation with NaBAF. Reactions were run for 6.5 h and then quenched and worked up as in the general procedure. The MA incorporation ratio was calculated from ^{1}H NMR analysis as done before in previous studies of MA-copolymers.[4] Samples were further characterized by SEC-MALS as described below. The catalyst TON was calculated using the average monomer

(42) Gottfried, A. C.; Brookhart, M. *Macromolecules* **2003**, *36*, 3085−3100.

molecular weight, based on the MA incorporation ratio using the formula

$$\mathrm{TON} = \frac{m}{n_c(M_{=}(1 - Ir) + M_{\mathrm{MA}}Ir)}$$

where m is the yield of polymer, n_c is the catalyst load, Ir is the incorporation ratio, and $M_{=}$ and M_{MA} are the molecular weights of ethylene and MA, respectively.

SEC-MALS Characterization of Polymers.[6,7] All the polymers were characterized by size-exclusion chromatography (SEC) coupled to a multiangle light scattering detector (MALS) for obtaining both polymer MW (M_n and M_w) and R_g. Measurements were made on highly dilute fractions eluting from a SEC consisting of a HP Aglient 1100 solvent delivery system/auto injector with an online solvent degasser, temperature-controlled column compartment, and an Aglient 1100 differential refractometer. A Dawn DSP 18-angle light scattering detector (Wyatt Technology, Santa Barbara, CA) was coupled to the SEC to measure both the MW and sizes for each fraction of the polymer eluted from the SEC column. A 30 cm column was used (Polymer Laboratories PLgel Mixed C, 5 μm particle size) to separate polymer samples. The mobile phase was THF, and the flow rate was 0.5 mL/min. Both the column and the differential refractometer were held at 35 °C. A 60 μL sample of a 2 mg/mL solution was injected into the column. ASTRA 4.7 from Wyatt Technology was used to acquire data from the 18 scattering angles (detectors) and the differential refractometer. The M_n and M_w data were obtained by following classical light scattering treatments.

Acknowledgment. We thank the National Science Foundation (DMR-0135233) and the University of California at Irvine for partial financial support. We thank the laboratories of Professors Richard A. Chamberlin, Larry E. Overman, Scott D. Rychnovsky, Kenneth J. Shea, and Keith A. Woerpel for use of lab instrumentation and chemicals.

OM048988J